Contents lists available at ScienceDirect

Chemical Engineering Research and Design

journal homepage: www.elsevier.com/locate/cherd

Hydrogen enrichment of fuels using a novel miniaturised chemical looping steam reformer

*Behdad Moghtaderi**

Priority Research Centre for Energy, Chemical Engineering, School of Engineering, Faculty of Engineering & Built Environment, The University of Newcastle, University Drive, Callaghan, NSW 2308, Australia

ABSTRACT

Experiments were conducted on the Fe_3O_4/FeO metal oxide system under pure methane and pure steam environments in a thermogravimetric analyser (TGA) and a prototype-miniaturised micro-reactor. Experimental results show that during a typical fuel oxidation step the concentration of methane in the product gas stream gradually decreases while Fe_3O_4 is being reduced to FeO. However, on or about a fractional conversion of 60% the slope of the CH_4 plot sharply increases due to catalytic effects of FeO on methane decomposition. Similarly, the H_2 plot associated with steam reforming step picks up rapidly and reaches a maximum of 98% at a fractional conversion of 30%. The conversion times of steam and fuel in the micro-reactor were generally shorter than conversion times obtained in the TGA system. The experimental results provided two vital pieces of information: (i) the chemical looping steam reforming cycle is technically viable, and (ii) the performance of the process at micro-scales needs to be further understood before high throughput miniaturised reformers could be designed and built.

Keywords: Chemical looping steam reforming; Microfluidics

1. Introduction

The hydrogen enrichment of gaseous and liquid fuels on-board of stationary and mobile combustion systems is a topic of significant interest in many applications such as internal combustion engines (ICE), liquid and/or gas fired boilers, gas turbines, and micro-combustors (for potential use in medical devices, military equipment, cell phones, notebook computers and other similar electronic devices). The interest in hydrogen enrichment of fuels is largely driven by the fact that addition of small quantities of hydrogen into a premixed fuel mixture can greatly extend the lean and dilution limits of the mixtures with simultaneous benefits of increasing the overall thermal efficiency and reducing emissions. For example, in the case of ICEs the hydrogen enrichment of the air/fuel mixture can improve the overall thermal efficiency of the engine by as much as 20% and lower its NO_x and CO_2 emissions by 98% and 20%, respectively (Jamal and Wyszynski, 1994; Schefer, 2003).

The improvements in thermal efficiency and emission reductions due to hydrogen enrichment can greatly help to reduce the greenhouse gas (GHG) footprints of many industrial sectors that primarily rely on combustion based systems. For instance, according to the International Energy Agency (IEA, 2005) the use of internal combustion engines in the transportation sector alone is responsible for 18.4% of the global CO_2 emissions and about 22% of the national GHG inventory in Australia. If the hydrogen enrichment concept is deployed across even 10% of the transportation sector, the global GHG emissions can be reduced by 100 million tonnes per year, which is equivalent of removing 20 million average cars off the roads each year.

While the concept of hydrogen enrichment of fuels in gas turbines (Schefer, 2003), boilers (Hsieh and Jou, 2007) or micro-combustors (Wang et al., 2010) has not been widely investigated, the concept has been demonstrated for gaseous and liquid fuels in ICEs (e.g. Collier, 2004; Collier et al., 1996; Erickson et al., 2006; Jamal and Wyszynski, 1994). However, because of the unresolved technical issues associated with on-board storage of hydrogen, a variety of on-board fuel reformers have been developed for in situ production of H_2 and implementation of the hydrogen enrichment concept in ICEs. The majority of these on-board systems incorporate conventional

* Tel.: +61 2 4985 4411; fax: +61 2 4921 6893.
E-mail address: Behdad.Moghtaderi@newcastle.edu.au
Received 12 March 2011; Received in revised form 7 June 2011; Accepted 14 June 2011
0263-8762/$ – see front matter © 2011 The Institution of Chemical Engineers. Published by Elsevier B.V. All rights reserved.
doi:10.1016/j.cherd.2011.06.012

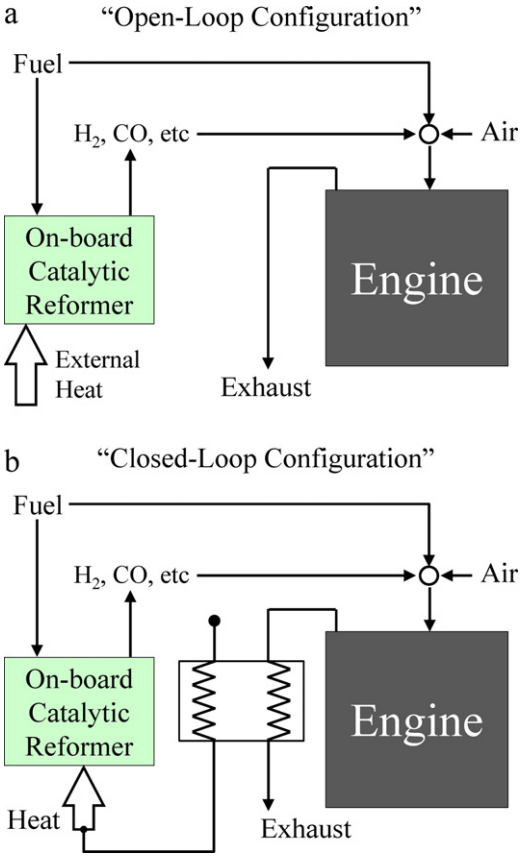

Fig. 1 – Schematic representation of hydrogen enrichment in ICEs, (a) open-loop configuration, and (b) closed-loop configuration.

catalytic reformers in an open-loop configuration where a secondary source of energy is employed for hydrogen production (Fig. 1a). Clearly, from energy efficiency point of view the open-loop configuration is not an attractive option and a closed-loop configuration is preferred because the hydrogen production can be achieved with minimum energy penalty using the waste heat from the exhaust stream (Fig. 1b). Despite its merits, even the closed-loop configuration has had a limited success and been demonstrated only in heavy duty ICEs for gaseous fuels (Collier, 2004; Collier et al., 1996). There are several reasons for the limited success of conventional closed-loop on-board fuel reformers chiefly among them:

- the low purity of the product gas stream in terms of its H_2 content;
- unwanted sudden changes in the rate and composition of the product gas stream due to perturbations in the waste heat recovery process under load, and;
- large physical dimensions and heavy weights of conventional catalytic reformers.

The fuel reforming technology under development at the University of Newcastle (Australia) is an attempt to resolve the above shortcomings by integrating the principles of chemical looping steam reforming (CLSR) and process miniaturisation into a unified platform (Moghtaderi, 2010a,b; Moghtaderi and Song, 2010). Chemical looping steam reforming with its inherent ability for CO_2 capture/separation would enable the fuel reformer to generate a pure stream of hydrogen and thereby avoid any fluctuations in the composition of the product gas stream (Fig. 2). Similarly, the implementation

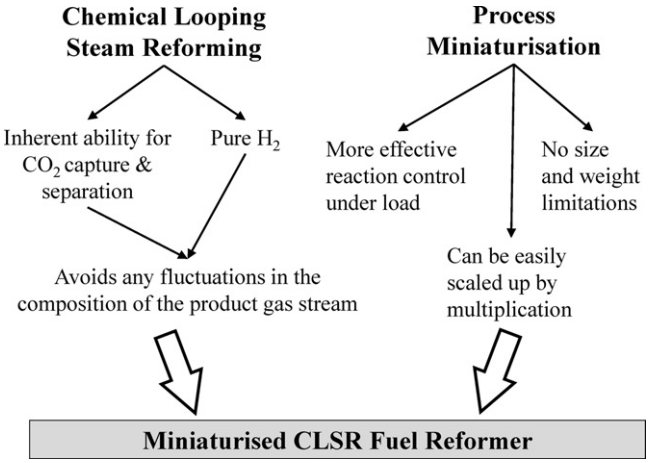

Fig. 2 – Basic features of integrated chemical looping steam reforming and process miniaturisation concepts.

of process miniaturisation principles (i.e. microfluidics and micro-technology concepts) would allow us to achieve a more effective control over reaction rates and hence the rate of hydrogen production under load (Fig. 2). In addition, miniaturised reformers do not have the size and weight limitations of conventional reformers and can be easily scaled up by multiplication (i.e. parallel scale-up) and be retrofitted to all existing (e.g. ICEs, gas turbines, boilers) and emerging (e.g. micro-combustors) combustion systems in the transportation and power generation sectors. This paper presents a preliminary assessment of the miniaturised CLSR concept and is part of a larger ongoing program of study at the University of Newcastle.

2. Miniaturised chemical looping stream reforming

2.1. *The miniaturised CLSR concept*

The working principle of the CLSR concept together with other chemical looping reforming (CLR) pathways has been shown schematically in Fig. 3. All CLR type processes are based on the cyclic reduction and oxidation of either oxygen carrier or CO_2 scavenger particles (Fig. 4), which are used to transport oxygen or CO_2 within the cycle. At macro-scales (large-scale), the CRL

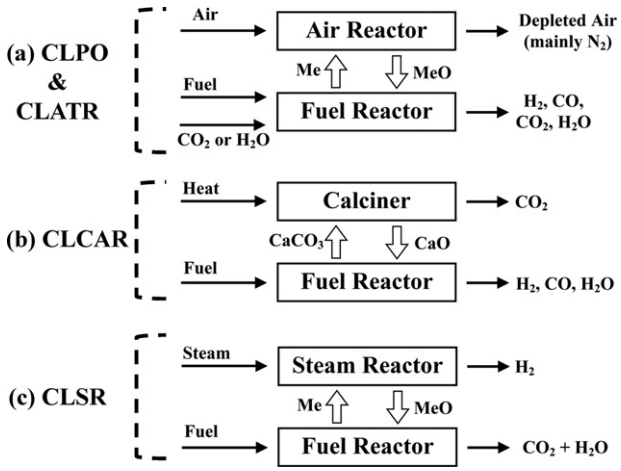

Fig. 3 – Alternative pathways for chemical looping reforming (note that MeO and Me denote metal oxide and reduced metal).

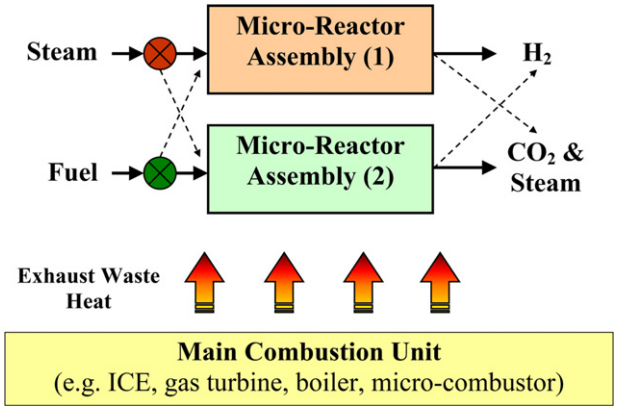

Fig. 4 – Schematic representation of the miniaturised CLSR fuel reformer.

Fig. 5 – Picture of a micro-reactor assembly.

processes are typically carried out by exchanging the carrier particles between two interconnected fluidised bed reactors.

The main goal in CLR processes is to produce hydrogen or synthesis gas (a mixture of H_2 and CO) rather than heat and power (Go et al., 2009; He et al., 2009; Shulman et al., 2009; Xiang and Wang, 2008; Abad et al., 2007; Rydén and Lyngfelt, 2006). For this reason, the air to fuel ratio is kept low to prevent the complete oxidation of fuel to CO_2 and water. As illustrated in Fig. 3, the major pathways for chemical looping reforming are chemical looping partial oxidation (CLPO) and auto-thermal reforming (CLATR; Fig. 3a), chemical looping CO_2 acceptor reforming (CLCAR; Fig. 4b); and chemical looping steam reforming (CLSR; Fig. 3c). In both CLPO and CLATR cases (Fig. 3a) the fuel is provided with sub-stoichiometric oxygen to generate synthesis gas. However, for CLATR a reformer gas (typically either steam or CO_2) is also introduced into the fuel reactor. In the CLCRA case (Fig. 3b) the cyclic carbonisation and calcination of a CO_2 scavenger, such as CaO, is used to improve the selectivity of hydrogen in the product gas stream. Finally, in CLSR (Fig. 3c) the fuel is completely oxidised and carrier particles are fully reduced in the fuel reactor. Reduced particles are then directed to the steam reactor where pure H_2 is produced by oxidisation or regeneration of particles with steam.

Among the above alternative pathways, the CLSR process is more attractive for on-board applications mainly because the production of hydrogen in CLSR is divided into two separate steps of "*fuel oxidation*" (i.e. carrier particle reduction) and "*steam reduction*" (i.e. carrier particle oxidisation). This allows the production of H_2 to proceed without any post-processing such as water gas shift reaction or pressure swing adsorption (Go et al., 2009). Also, in terms of energy demand and thereby cost effectiveness, the CLSR process is very appealing, as it requires relatively low levels of energy input (note: reaction between steam and carrier particles is exothermic). Unfortunately, the CLSR concept as described here cannot be directly applied to on-board systems because of:

(i) relatively large physical dimensions of conventional fluidised bed reactors often used in chemical looping applications;
(ii) difficulties associated with the circulation of solids between interconnected fluidised bed reactors, and;
(iii) relatively slow reaction rates and conversion efficiencies of carrier particles.

The above drawbacks can be effectively resolved through process intensification, process miniaturisation and the use of fixed-bed reactors. These goals can be simultaneously accomplished if the CLSR reactions are carried out within a network of fixed bed micro-reactors each packed with metal oxide particles and fitted with a manifold switching system for periodic changeover of feed stream from fuel to steam. In this arrangement, the reacting gases rather than carrier particles are exchanged. The enhancement of heat and mass transfer processes in such a miniaturised system is largely due to the use of the micro-reactor networks, which generally offer (Ehrfeld et al., 2000):

(i) large surface-to-volume-ratios (i.e. large contact area between reactants which ultimately increases the reaction rates and shortens the required residence time);
(ii) low pressure drops due to laminar flow regime;
(iii) controllable back mixing and residence time distribution;
(iv) high volumetric productivity;
(v) increased safety due to small material hold-up;
(vi) ease of scale-up, and;
(vii) low operating costs.

2.2. *The miniaturised CLSR reformer*

The miniaturised CLSR based fuel reformer developed as part of this study is quite novel and to the best of author's knowledge has neither been investigated in the past nor being studied anywhere in the world. The proposed system, as shown schematically in Fig. 4, incorporates a pair of identical micro-reactor assemblies (Fig. 5) each comprising 272 micro-reactors packed with metal oxide particles. Unlike conventional chemical looping systems, carrier particles are not circulated between the two reactor assemblies and the cycle is completed by switching over the steam and fuel inlet streams from one reactor assembly to the other. Each assembly, therefore, functions periodically as a fuel reactor and a steam reactor. The changeover of the flow is achieved using a manifold switching system (dashed arrows in Fig. 4). Fuel heater and steam generator units have also been fitted to the reformer upstream of the manifold switching system (not shown in Fig. 4). The fuel heater is used to pre-heat the fuel and/or convert any liquid fuel to vapour. The required fuel for the process is obtained from the main combustion system to which the chemical looping reformer is attached (e.g. an ICE). The pure H_2 produced by the fuel reformer is directed to the main combustion system for on-board use. The mixture of CO_2

and steam, which is inherently separated from H_2 in the product gas stream, can be further processed in several alternative ways. For example, steam can be separated from CO_2 by condensation in a heat exchanger where fuel is pre-heated. The separated CO_2 can be then exhausted or captured by chemicals in an absorber. The condensed water can be also recycled for steam generation. Alternatively, the CO_2 in the CO_2/steam mixture can be separated first in an absorber and then the CO_2 free mixture is recycled to the CLSR process.

Typically, the fuel oxidation reaction (i.e. metal oxide reduction) in the fuel reactor is endothermic while the steam reduction (i.e. metal oxide oxidation) in the steam reactor is exothermic. For many potentially suitable metal oxide species, the overall chemical looping reforming process is not thermally balanced and is typically endothermic. For instance, in the case of Fe_3O_4/FeO metal oxide system with a gaseous fuel such as methane, the endothermicity of the overall reaction is about 389 kJ/mol (see reactions (1) and (2) below).

$$\text{(Reduction)}\quad 4Fe_3O_4 + CH_4 \rightarrow 12FeO + CO_2 + 2H_2O$$

$$\Delta H_{298} = 463.7\ \text{kJ/mol} \qquad (1)$$

$$\text{(Oxidation)}\quad 3FeO + H_2O \rightarrow Fe_3O_4 + H_2$$

$$\Delta H_{298} = -74.7\ \text{kJ/mol} \qquad (2)$$

Therefore, heat must be supplied to the process to maintain a smooth operation. Additional heat is also required to maintain the operation of the steam generator and fuel heater. Given that the proposed fuel reformer is for on-board applications and noting that the exhaust gases from such systems carry considerable amount of waste heat (e.g. about 60% of the input energy in ICEs), in the proposed miniaturised CLSR concept the heat source is considered to be the recycled exhaust gas stream.

The design of the micro-reactor assemblies of the fuel reformer is based the so called plate/stack architecture where micro-reactors are embedded in a number of planner structures (i.e. plates) stacked on top of each other to form the reactor assembly. To achieve a desired throughput, the reformer can be scaled up or down simply by changing the number of reactor plates in each stack or alternatively the number of pairs of micro-reactor assemblies. The author has successfully used these types of plate/stack systems in his past studies (Moghtaderi, 2007; Djenidi and Moghtaderi, 2006; Moghtaderi et al., 2006). The configuration most suited to the miniaturised CLSR concept is shown in Fig. 6. Zigzag shape reactors are used in this configuration to provide a better contact between particles and reacting gases and, hence, optimise the residence time and physical dimensions. The miniaturised reactor assembly shown in Fig. 5 incorporates the above configuration and comprises 272 zigzag shape micro-reactors (0.05 m long with a cross sectional area of 200 μm × 100 μm) organised in 16 reactor plates each with 17 micro-reactors.

3. Experimental

Experiments were conducted at 700 °C, 800 °C and 900 °C on magnetite (Fe_3O_4) and its reduced form (wuestite or FeO) in a thermogravimetric analyser (TGA) as well as a prototype miniaturised micro-reactor plate. The selection of Fe_3O_4/FeO

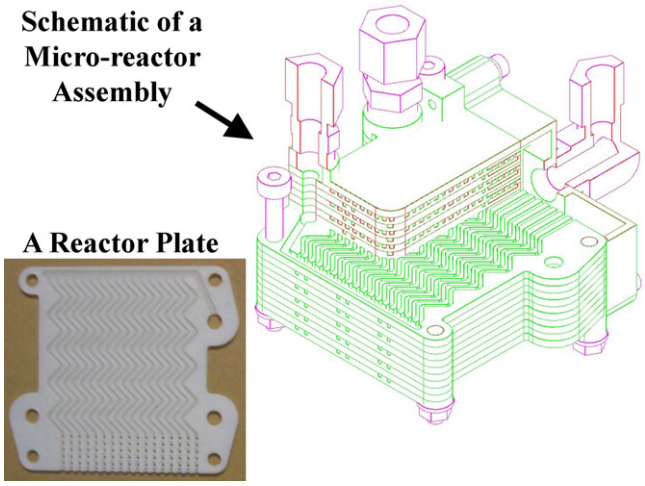

Fig. 6 – Schematic cutout view of a micro-reactor assembly.

oxide system was due to its good thermodynamic characteristics, low cost and minimum environmental impact. The preparation of magnetite metal oxide samples begun by the direct mixing of a commercial Fe_3O_4 powder (Sigma–Aldrich) with alumina powder (Sigma–Aldrich) at a 3:2 carrier/support weight ratio. The use of carrier support was important since past studies (e.g. Moghtaderi and Song, 2010) have revealed that pure carrier particles are unsuitable for extended use in chemical looping systems, primarily because their reactivity, chemical stability, and mechanical durability are relatively low. Inert support materials, such as silica, alumina, yttria-stabilised zirconia (YSZ), kaolin and various metal aluminates were used in past investigations to enhance the mechanical strength and reactivity of carrier particles by improving particle porosity and surface characteristics. The 3:2 carrier/support ratio was selected based on our past experience with similar materials (Moghtaderi and Song, 2010).

Once the carrier/support mix was made, distilled water was added to form a paste. For miniaturised micro-reactor experiments the internal surfaces of the reactor plates were coated with a 1 μm layer of the past. The coated plates were then placed in an oven at 105 °C for 36 h to dry the past and free up the capillary water. The dry paste was then calcined at 900 °C under nitrogen for about 5 h by placing reactor plates in a high temperature furnace. The necessary carrier particles for TGA tests were prepared by drying the paste in an oven at 105 °C for 36 h and then calcining the dry past at 900 °C under nitrogen for about 5. The resulting material after the calcination process was pulverised in a ball mill and sieved to a particle size range of 20–40 μm.

The quality of the final products were evaluated using X-ray diffraction (XRD) and transmission electron microscopy (TEM) and SEM methods to determine the distribution of metal active sites on the surface and within the carrier particles, respectively. Fig. 7 shows the XRD spectra pattern for fresh magnetite samples prepared in this study. The peaks are not very sharp suggesting that a well-crystalline structure has not been fully formed. Fig. 8 illustrates the TEM image of an oxygen carrier sample applied to a micro-reactor panel. The average particle size appears to be about 200 nm. SEM analysis revealed that a cluster of similar size particles typically forms a single particle unit of 20–40 μm used in TGA experiments.

TGA experiments were performed in two separate steps in the batch mode (i.e. fuel oxidation and steam reduction). The fuel oxidation step (i.e. reduction of Fe_3O_4 to FeO) was carried

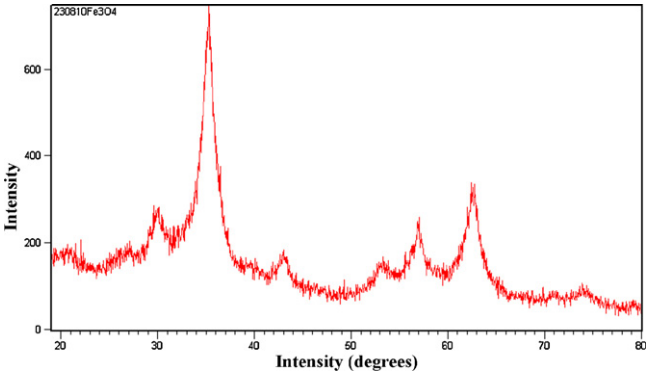

Fig. 7 – XRD spectra for magnetite oxygen carrier samples.

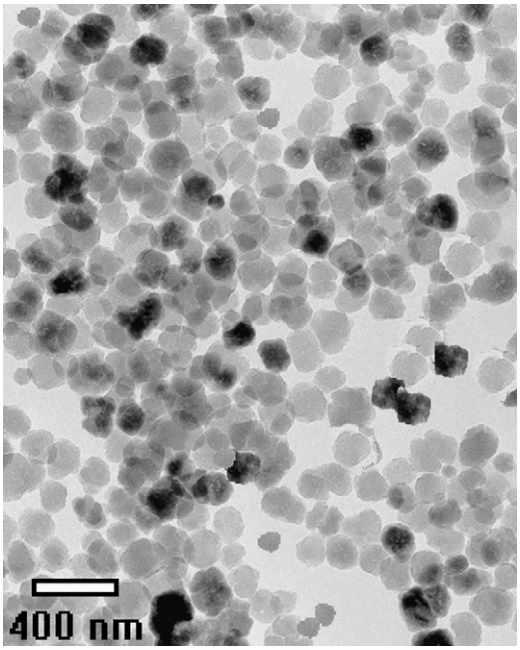

Fig. 8 – TEM image of magnetite particles in a micro reactor channel.

out in pure methane while the steam reduction step was conducted in an environment of pure steam. A nitrogen purge was used between each step to flush out residual gases. Measurements of instantaneous weight loss were made for a range of different cases. Several cycles (i.e. pairs of fuel oxidation and steam reduction experiments) were repeated in each case to ensure the accuracy of collected data. A micro-GC was used to quantify the concentration of gaseous species in the TGA outlet.

The experimental set-up used in micro-reactor studies as shown in Fig. 9 consisted of:

(i) a gas pre-heater;
(ii) a 0.05 m × 0.05 m × 0.1 m electrical heated chamber;
(iii) a single stack micro-reactor assembly comprising a cover plate and a reactor plate with 17 zigzag shape micro-reactors (0.05 m long with a cross sectional area of 200 μm × 100 μm) engraved in a stainless steel plate;
(iv) a water-cooled heat exchanger;
(v) a gas analysis train comprising a drierite column and a high-resolution gas chromatograph;
(vi) a set of syringe pumps, and;
(vii) a data acquisition/process control unit.

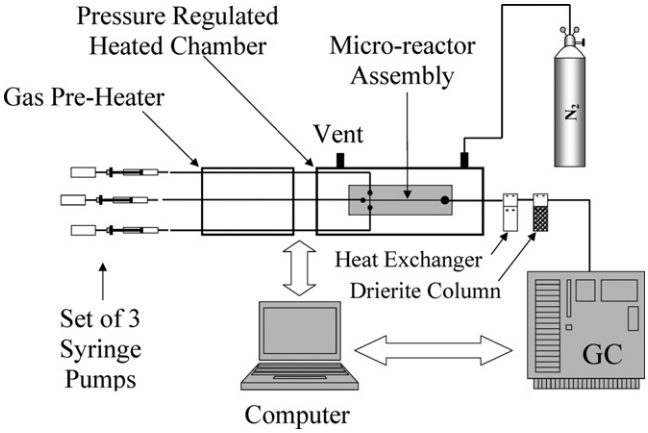

Fig. 9 – Micro-reactor experimental setup.

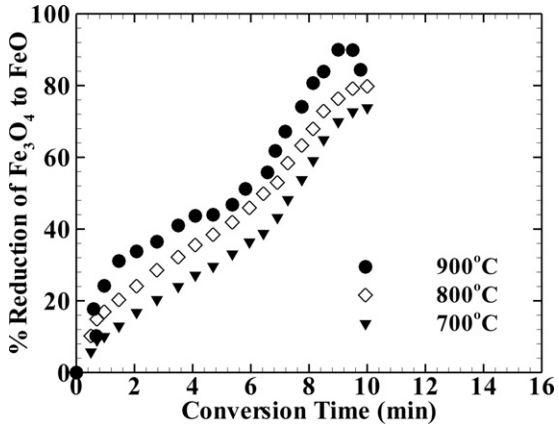

Fig. 10 – Fractional conversion of Fe_3O_4 to FeO during reduction in TGA.

4. Results and discussion

The summary of experimental results obtained as part of this study is presented in this section. While Figs. 10–12 deal with TGA experiments, Figs. 13 and 14 have been dedicated to micro-reactor studies. Figs. 10 and 11 illustrate plots of metal oxide conversion against conversion time in TGA for reduction and oxidation reactions, respectively.

As can be seen from Fig. 10, fractional reduction of Fe_3O_4 in an environment of methane increases relatively rapidly at the beginning of the reduction process as Eq. (1) proceeds at reasonably high rates. The reaction rate however decreases as

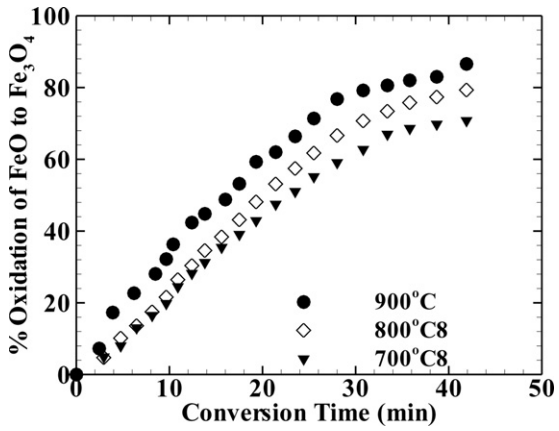

Fig. 11 – Fractional conversion of FeO to Fe_3O_4 during oxidation in TGA.

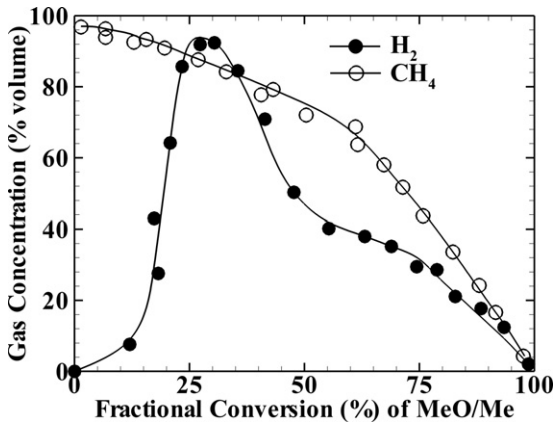

Fig. 12 – Concentration of gaseous products versus fractional conversion at 900 °C.

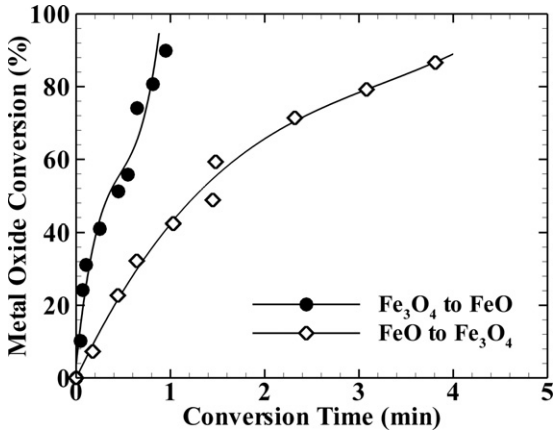

Fig. 13 – Fractional conversion of metal oxides during reduction and oxidation steps in the micro-reactor setup at 900 °C.

more and more FeO phase is formed and the reduction process shifts towards the partial oxidation of methane, Eq. (3), (note that reduction of FeO by H_2 and CO is thermodynamically unfavourable). Beyond a fractional conversion of 0.6, the level of FeO phase would be high enough to cause significant catalytic decomposition of methane. As a result solid carbon and more H_2 are formed which are both fully oxidised by Fe_3O_4 leading to an increased level of Fe_3O_4 reduction. However, further increase in the rate of reaction and thereby more Fe_3O_4 conversion causes an imbalance between the rate of solid carbon formation and consumption. This, in turn, leaves carbon

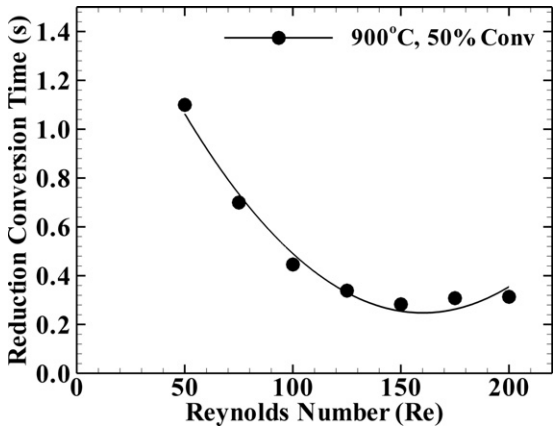

Fig. 14 – Conversion time versus *Re* in the micro-reactor setup.

deposits on the surfaces of metal oxide particles degrading their reactivity (this has been visually verified). As a result, the sample weight increases and the overall reaction rate sharply plunges.

$$Fe_3O_4 + CH_4 \rightarrow 3FeO + CO + 2H_2 \quad \Delta H_{298} = 280.9\,\text{kJ/mol} \quad (3)$$

As shown in Fig. 11, the oxidation of FeO to Fe_3O_4 under an environment of steam is much slower than its corresponding reduction reaction under methane. Note the conversion time for oxidation is almost 4 times longer than reduction time for all temperatures investigated here. At a temperature of 900 °C, the oxidation rate is initially fast and constant but levels off at conversions greater than 80%.

Fig. 12 illustrates the plots of fractional conversion of metal oxide particles versus the concentration of H_2 and CH_4 in the product stream obtained from TGA experiments. The open symbols represent the data corresponding to reduction of Fe_3O_4 to FeO (i.e. CH_4 oxidation step) whereas the solid symbols show the data obtained from the oxidation step (i.e. FeO to Fe_3O_4 in steam, Eq. (2)). As can be seen from the methane plot, the concentration of methane in the product gas gradually decreases while Fe_3O_4 is being transformed to FeO. However, on or about a fractional conversion of 60% the slope of the CH_4 plot sharply increases. This profound change can be attributed to catalytic effect of FeO on methane decomposition, which was noted earlier. Similarly, the H_2 plot picks up rapidly and reaches its maximum value of 98% at a fractional conversion of 30%. Beyond this point, however, the concentration of hydrogen in the product gas stream diminishes until all FeO particles have been oxidised to Fe_3O_4. This particular trend can be also attributed to the fact that unlike FeO, magnetite (Fe_3O_4) does not have much of a catalytic effect.

Given the crystalline structure of magnetite and wustite, the morphological evolutions of iron based oxygen carriers after repeated chemical looping cycles is an important consideration in the context of the present study. The oxidation of wustite to magnetite results in distinct changes in the morphology of magnetite (Wagner et al., 2006). These changes depend on structural properties of parent wustite and oxidation conditions. The nucleation of magnetite at high temperatures is quite different than at low temperatures. However, given that in the present study the oxidation experiments were typically run at relatively high temperatures between 700 °C and 900 °C, the morphological characteristics (e.g. grain size, grain shape, etc.) of magnetite samples produced at these temperatures were found to be very similar and independent of the temperature. There was, however, a widening of the half-width of the XRD peaks as a function of number of cycles, indicating a general degradation of the crystalline structure (i.e. less order). These are believe to be partly responsible for deactivation of oxygen carriers which typically occured after about 2500 cycles.

Fig. 13 illustrates the fractional conversion of FeO and Fe_3O_4 under reducing and oxidising environments in the micro-reactor setup ($Re = 100$ for steam and methane). The fractional conversion was calculated based on the initial (W_0), instantaneous (W_t) and final (W_f) weights using the following equation:

$$X = \frac{W_0 - W_t}{W_0 - W_f} \quad (4)$$

The solid symbols in Fig. 13 represent the reduction process while the open symbols show the oxidation results. While

both plots show striking resemblance with their TGA counterparts shown in Figs. 10 and 11, the corresponding conversion times for micro-reactor results are much shorter. Generally, the micro-reactor conversion times appear to be 10% of those obtained from TGA experiments. This is a clear indication that reasonable levels of process intensification can be achieved by miniaturising the chemical looping steam reforming process. However, yet again the rate of oxidation (conversion of FeO to Fe_3O_4 under steam) seems to be much slower than the rate of reduction. This imbalance between the rate of reactions from Fe_3O_4 to FeO and FeO to Fe_3O_4 is not unique and may occur for other metal oxide species. The imbalance, however, can be an impediment to the operation of the system if not properly alleviated. In conventional chemical looping systems different solid inventories and, thereby, different size reactors are employed to resolve the imbalance between MeO/Me and Me/MeO reaction rates. The effective management of this imbalance in the CLSR miniaturised reformer can be achieved by multi-stage operation to ensure continuous production of hydrogen. For example, in the case of Fe_3O_4/FeO the steam reduction step can be carried out in the relevant micro-reactor assembly in two consecutive stages each having a time span equal to 50% of the residence time (i.e. conversion time associated with the slower fuel oxidation step) and incorporating half of the reactor-plates in the assembly. The slower fuel oxidation step can be performed in a single stage.

Fig. 14 shows the plot of conversion time during reduction versus the Reynolds number; highlighting the impact of the gas velocity (in this case methane) on the overall rate of reaction and thereby conversion time. The data reported in Fig. 14 correspond to 50% conversion from Fe_3O_4 to FeO at 900 °C in the micro-reactor setup (Fig. 9).

Clearly, the reaction time drops off (i.e. enhancement of reaction rate) when the velocity and hence the *Re* of the reacting gas is increased although at $Re \geq 150$ the trend is reversed. While this reversal is not fully understood, the gas composition measurements show higher concentrations of H_2 in the product gas stream when the *Re* is increased to levels greater than 150. This is an indication that H_2 and solid carbon formed due to catalytic decomposition of methane by FeO are prematurely taken out of the reaction zone before they have any chance of reacting with un-reacted Fe_3O_4 particles.

5. Conclusions

A comprehensive series of experiments was carried out to assess the technical viability of the miniaturised chemical looping steam reforming for hydrogen enrichment of fuels. The experimental results provided two vital pieces of information: (i) the chemical looping steam reforming cycle is technically viable, and (ii) the performance of the process at micro-scales needs to be further understood before high throughput miniaturised reformers could be designed and built. This is the subject of our ongoing investigations.

Acknowledgements

The author wishes to acknowledge the financial support provided to this project by the University of Newcastle (Australia).

References

Abad, A., García-Labiano, F., de Diego, L.F., Gayán, P., Adánez, J., 2007. Reduction kinetics of Cu–Ni–, and Fe-based oxygen carriers using syngas ($CO + H_2$) for chemical-looping combustion. Energy Fuels 21, 1843–1853.

Collier, K., 2004. HCNG, the proven low emissions technology for internal combustion engines. In: Indian International SAE Conference , New Delhi, India, paper number 082.

Collier, K., Hoekstra, R., Mulligan, N., Jones, C., Hahn, D., 1996. Untreated exhaust emissions of a hydrogen-enriched CNG production engine conversion. SAE 960858-Int. Cong. & Expo., Detroit, MI, February.

Djenidi, L., Moghtaderi, B., 2006. Numerical investigation of laminar mixing in a coaxial microreactor. J. Fluid Mech. 568, 223–242.

Ehrfeld, W., Hessel, V., Loww, H., 2000. Microreactors: New Technology for Modern Chemistry. Wiley-VCH.

Erickson, P., Vernon, D., Jordan, E., Collier, K., Mulligan, N., 2006. Low NOx operation and recuperation of thermal and chemical energy through hydrogen in internal combustion engines. In: Proceedings of the 16th Annual Hydrogen Conference of the National Hydrogen Association, 1–11, March 29–April 1 , Washington, DC.

Go, K.S., Son, S.R., Kim, S.D., Kang, K.S., Park, C.S., 2009. Hydrogen production from two-step steam methane reforming in a fluidized bed reactor. Int. J. Hydrogen Energy 34, 1301–1309.

He, F., Wei, Y., Li, H., Wang, H., 2009. Synthesis gas generation by chemical-looping reforming using Ce-based oxygen carriers modified with Fe, Cu, and Mn oxides. Energy Fuels 23, 2095–2102.

Hsieh, S.C., Jou, C.J.G., 2007. Reduction of greenhouse gas emission on a medium-pressure boiler using hydrogen-rich fuel control. Appl. Therm. Eng. 27, 2924–2928.

International Energy Agency Report, 2005. Carbon Dioxide Emissions by Economic Sector.

Jamal, Y., Wyszynski, M.L., 1994. On-board generation of hydrogen-rich gaseous fuel—A review. Int. J. Hydrogen Energy 19 (7), 557–572.

Moghtaderi, B., 2007. Effect of enhanced mixing on partial oxidation of CH_4 in a novel micro-reactor. Fuel 86, 469–476.

Moghtaderi, B., 2010a. A novel miniaturised fuel reformer for on-board hydrogen enrichment of gaseous and liquid fuels in combustion systems. In: Proceedings of Chemeca 2010 , Adelaide, Australia.

Moghtaderi, B., 2010b. Application of chemical looping concept for air separation at high temperatures. Energy Fuels 24, 190–198.

Moghtaderi, B., Shames, I., Djenidi, L., 2006. Microfluidic characteristics of a multi-holed baffle plate micro-reactor. Int. J. Heat Fluid Flow 27, 1069–1077.

Moghtaderi, B., Song, H., 2010. Reduction properties of physically mixed metallic oxide oxygen carriers in chemical looping combustion. Energy Fuels 24, 5359–5368.

Rydén, M., Lyngfelt, A., 2006. Using steam reforming to produce hydrogen with carbon dioxide capture by chemical-looping combustion. Int. J. Hydrogen Energy 31, 1271–1283.

Schefer, R.W., 2003. Hydrogen enrichment for improved lean flame stability. Int. J. Hydrogen Energy 28, 1131–1141.

Shulman, A., Cleverstam, E., Mattisson, T., Lyngfelt, A., 2009. Manganese/iron, manganese/nickel, and manganese/silicon oxides used in chemical-looping with oxygen uncoupling (CLOU) for combustion of methane. Energy Fuels 23, 5269–5275.

Wagner, D., Devisme, O., Patisson, F., Ablitzer, D., 2006. A laboratory study of the reduction of iron oxides by hydrogen, TMS. In: Kongoli, F., Reddy, R.G. (Eds.), Proceedings of the Sohn International Symposium, vol. 2. 27–31 August 2006, San Diego, USA, pp. 111–120.

Wang, Y., Zhou, Z., Yang, W., Zhou, J., Liu, J., Wang, Z., Cen, K., 2010. Combustion of hydrogen-air in micro combustors with catalytic Pt layer. Energy Convers. Manage. 51, 1127–1133.

Xiang, W., Wang, S., 2008. Investigation of gasification chemical looping combustion combined cycle performance. Energy Fuels 22, 961–966.